

Stable three-dimensional optical solitons supported by competing quadratic and self-focusing cubic nonlinearities

D. Mihalache,^{1,2,3} D. Mazilu,^{2,3} B. A. Malomed,⁴ F. Lederer,³ L.-C. Crasovan,^{1,2} Y. V. Kartashov,¹ and L. Torner¹

¹*ICFO–Institut de Ciències Fòniques, Mediterranean Technology Park, 08860 Castelldefels (Barcelona), Spain*

²*Horia Hulubei National Institute for Physics and Nuclear Engineering (IFIN-HH),*

407 Atomistilor, Magurele-Bucharest 077125, Romania

³*Institute of Solid State Theory and Theoretical Optics, Friedrich-Schiller Universität Jena, Max-Wien-Platz 1, D-077743 Jena, Germany*

⁴*Department of Interdisciplinary Studies, Faculty of Engineering, Tel Aviv University, Tel Aviv 69978, Israel*

(Received 8 May 2006; revised manuscript received 28 June 2006; published 12 October 2006)

We show that the quadratic ($\chi^{(2)}$) interaction of fundamental and second harmonics in a bulk dispersive medium, combined with self-focusing cubic ($\chi^{(3)}$) nonlinearity, give rise to stable three-dimensional spatiotemporal solitons (STSs), despite the possibility of the supercritical collapse, induced by the $\chi^{(3)}$ nonlinearity. At exact phase matching ($\beta=0$), the STSs are stable for energies from zero up to a certain maximum value, while for $\beta \neq 0$ the solitons are stable in energy intervals between finite limits.

DOI: [10.1103/PhysRevE.74.047601](https://doi.org/10.1103/PhysRevE.74.047601)

PACS number(s): 42.65.Tg, 42.65.Sf

Optical solitons (temporal, spatial, and spatiotemporal) are at the core of the current research trends in nonlinear optics [1,2]. In many physically relevant models, which are not integrable, these are “solitary waves,” rather than solitons in the mathematically rigorous meaning of the word but, nevertheless, it has become common to use the term “soliton” in the loose sense. In particular, spatiotemporal solitons (STSs), also known as “light bullets” [3], have attracted a great deal of attention in recent years, as reviewed in Ref. [4]. These are multidimensional pulses, which maintain their shape in the longitudinal (temporal) and transverse (spatial) directions due to the balance between the group-velocity dispersion (GVD), diffraction, and nonlinear self-phase modulation. However, solitons in media with the cubic self-focusing nonlinearity, which obey the nonlinear Schrödinger (NLS) equation, are unstable in two and three dimensions (2D and 3D), due to the possibility of collapse in the same model [5]. Several ways to arrest the collapse and stabilize STSs were considered, such as periodic alternation of focusing and defocusing layers [6] and generalizations of this setting [2], dispersion management in 2D waveguides [7], lattice potentials in various forms [8], and the use of media exhibiting saturable [9] or quadratic ($\chi^{(2)}$) [10] nonlinearities. Despite the great progress in theoretical studies, the only successful experiment in this field was, thus far, the creation of quasi-(2+1)D STSs in bulk samples of $\chi^{(2)}$ materials [4,11].

A natural setting for the making of stable multidimensional solitons is provided by competing nonlinearities, such as combinations of cubic-quintic (CQ) [12,13] and quadratic-cubic ($\chi^{(2)}:\chi^{(3)}$) types [14,15]. In most cases [12,13,15], the competing nonlinearities were considered in terms of stabilization of spinning solitons, as the fundamental (zero-vorticity) multidimensional solitons are stable in $\chi^{(2)}$ media without the addition of $\chi^{(3)}$ nonlinearity [10], but spinning solitons are unstable in the same case [16]. In these settings, it was assumed that the higher nonlinear term, i.e., the quintic one in the CQ model, or the cubic term in the $\chi^{(2)}:\chi^{(3)}$ system, was self-defocusing, otherwise the model would give rise to collapse, and it was tacitly conjectured that the soli-

ton’s stability is not compatible with collapse. On the other hand, in works that considered cylindrically symmetric zero-vorticity (2+1)D spatial solitons in the bulk medium it was concluded that the combination of $\chi^{(2)}$ and *self-focusing* $\chi^{(3)}$ nonlinearities allows the existence of stable solitons of this type [17] (see also Ref. [18]). Further, both numerical simulations and experimental results reported in Ref. [11] demonstrate that 2D STSs may be stable too in a medium of the same type. In addition, it was recently demonstrated that a 1D model with the CQ nonlinearity, in which *both* cubic and quintic terms are self-focusing (such a model applies to Bose-Einstein condensation with attractive interactions between atoms), also gives rise to a family of stable solitons, despite the possibility of collapse in the respective Gross-Pitaevskii equation [19].

In fact, the coexistence of stable solitons with collapse in the abovementioned examples is not very surprising, as the respective models give rise to the critical collapse only, which is a regime observed exactly at the border between collapsing and noncollapsing model [5] (the critical collapse is simultaneously called strong, as the collapsing core involves a finite share of the initial energy, while, in the supercritical situation, the collapse is weak, as the share of the initial energy remaining in the collapsing core is vanishingly small, since the violent character of the collapse dynamics in this case leads to ejection of energy from the self-compressing core [5,20]). A challenging issue is whether three-dimensional STSs may be stable in the presence of the supercritical collapse, which actually implies consideration of the $\chi^{(2)}:\chi^{(3)}$ model in three dimensions, with the self-focusing cubic term. The model of this type is the most relevant one to optics, as it is difficult to find a medium combining the second-harmonic generation and negative Kerr coefficient, while the self-focusing Kerr nonlinearity is a common feature of $\chi^{(2)}$ media [4,11]. The objective of the present work is to demonstrate that families of stable 3D optical STSs are possible in media combining $\chi^{(2)}$ and self-focusing $\chi^{(3)}$ nonlinearities. This result can be understood, as the $\chi^{(2)}$ nonlinearity plays a dominant role if the soliton’s amplitude is small enough, and it is known that the $\chi^{(2)}$

model proper supports stable 3D solitons [4] (this was first demonstrated as early as in 1981, in the model with zero mismatch [21]). The solitons are expected to lose their stability at larger values of their energy (amplitude), where the $\chi^{(3)}$ nonlinearity dominates, driving the system toward the collapse.

Next we briefly present the physical model and the governing equations and then we report the basic numerical results for the existence and stability of soliton families, the latter being determined through computation of stability eigenvalues for perturbation modes. Direct numerical simulations confirm the predictions for the stability, and demonstrate that stable solitons readily self-trap from arbitrary initial pulses.

The general $\chi^{(2)}:\chi^{(3)}$ model relevant for the 3D case was elaborated in Ref. [15]. It can be used for the present purpose, by reversing the sign in front of the $\chi^{(3)}$ terms

$$iu_Z + (1/2)(u_{XX} + u_{YY} + u_{TT}) + u^*v + (|u|^2 + 2|v|^2)u = 0,$$

$$iv_Z + (1/4)(v_{XX} + v_{YY} + \sigma v_{TT}) - \beta v + u^2 + 2(2|u|^2 + |v|^2)v = 0. \quad (1)$$

Here, u and v are local amplitudes of the fundamental-frequency (FF) and second-harmonic (SH) waves with phase mismatch β between them, T , (X, Y) , and Z are the reduced time, two transverse spatial coordinates, and propagation distance, and the $\chi^{(2)}$ and $\chi^{(3)}$ coefficients can be normalized as set in the equations. Equations (1) assume different GVD coefficients at the two harmonics, with ratio σ between them [10] (the GVD coefficient in the equation for the FF component is normalized to be 1). Due to the invariance with respect to spatial rotations in the 3D space, Eqs. (1) feature invariance with respect to the ‘‘spatial Galilean transform.’’ On the contrary, the Galilean invariance proper, with respect to the temporal transformation $\tilde{T} = T - cZ$ with an arbitrary real walk-off parameter c , does not take place unless $\sigma = 1$ in Eqs. (1) [18]. The latter fact implies that generation of a family of ‘‘temporally walking’’ solitons in the case of $\sigma \neq 1$ is, by itself, a nontrivial problem. For 1D solitons, this problem was considered in detail in Ref. [22].

Stationary fundamental-soliton solutions to Eqs. (1) are looked for in the usual form $u = U(r, T)\exp(ikZ)$, $v = V(r, T)\exp(2ikZ)$, with amplitudes U and V obeying the equations

$$(1/2)(U_{rr} + r^{-1}U_r + U_{TT}) - kU + U^*V + (|U|^2 + 2|V|^2)U = 0,$$

$$(1/4)(V_{rr} + r^{-1}V_r + \sigma V_{TT}) - (2k + \beta)V + U^2 + 2(2|U|^2 + |V|^2)V = 0. \quad (2)$$

Equations (1) conserve the total energy $E = \iiint (|u|^2 + |v|^2)dXdYdT$, Hamiltonian H , and three components of the momentum [1]. From dependence $E = E(k)$ for the families of stationary solitons, one can try to predict their stability on the basis of the Vakhitov-Kolokolov (VK) criterion [5,23], $dE/dk > 0$, which is a necessary stability condition, securing the absence of instability eigenmodes with real eigenvalues. In Fig. 1 we summarize the output of extensive numerical

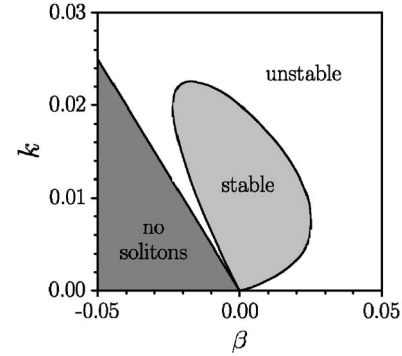


FIG. 1. Numerically found domains of the existence and stability of the spatiotemporal solitons for $\sigma = 1$.

calculations aimed to identify domains of the existence and stability of fundamental STSs in the parameter plane (k, β) . We start with the case of the spatiotemporal isotropy $\sigma = 1$ (a typical example of the situation with $\sigma \neq 1$ is shown below in Fig. 3). It is seen from Fig. 1 that the stability domain is asymmetric with respect to the mismatch parameter β ; at $\beta < 0$, the stability region expands to larger k , whereas at $\beta > 0$ the stability region shrinks in comparison with its counterpart for $\beta = 0$.

In Fig. 2, we display curves $E = E(k)$ and $H = H(E)$ for one-parameter families of the soliton solutions. A noteworthy feature of these dependences is that the 3D solitons exist at exact phase matching ($\beta = 0$) and at positive mismatch for any $k > 0$, whereas at $\beta < 0$ they exist only above a certain cutoff value $k_{CO} = -\beta/2$ (see also Fig. 1). We observe that the

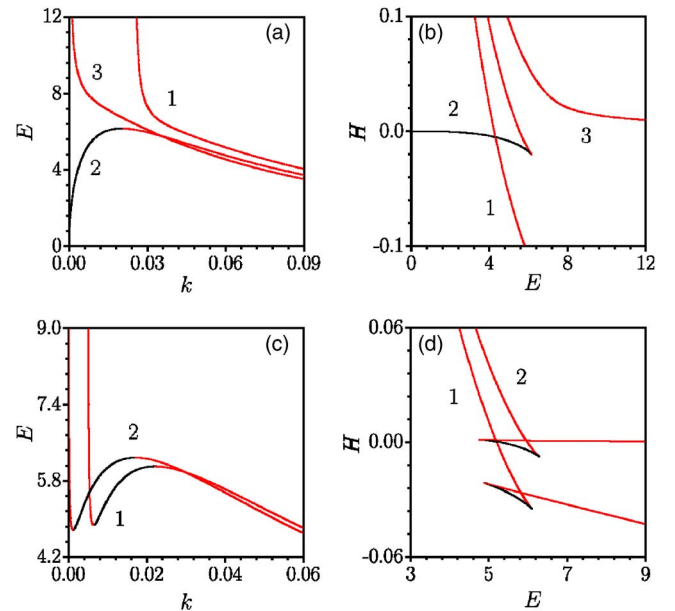


FIG. 2. (Color online) Characteristics of numerically found spatiotemporal soliton families for $\sigma = 1$. (a), (c) Energy E vs wave number k ; (b), (d) Hamiltonian vs E . In panels (a) and (b), labels 1, 2, and 3 correspond to $\beta = -0.05$, $\beta = 0$, and $\beta = 0.05$, respectively. In (c) and (d), labels 1 and 2 correspond to $\beta = -0.01$ and $\beta = 0.01$. Red (dark grey) and black lines depict unstable and stable soliton branches, respectively.

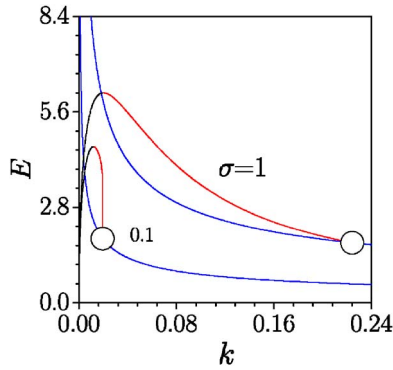


FIG. 3. (Color online) Energy E vs wave number k for soliton families at two values of the GVD ratio σ , and for $\beta=0$ (zero mismatch). Red (dark grey) and black lines depict unstable and stable solution branches, respectively, while blue (light grey) lines represent unstable 3D solitons in the corresponding $\chi^{(3)}$ medium.

stability of the solitons precisely obeys the VK criterion $dE/dk > 0$, despite the fact that, in more general situations (actually, for spinning solitons), this criterion is not a sufficient one. The method of the stability analysis is explained below. At exact phase-matching ($\beta=0$), the STSs are stable for energies from zero up to a certain maximum value, $E_{\max} \approx 6.2$, and the Hamiltonian-versus-energy (H - E) diagram displays a single cuspidal point, whereas for moderate finite values of β (either positive or negative ones) the solitons are stable in intervals of energy between finite limits, and the respective H - E diagrams feature a characteristic *swallowtail* shape, with two cuspidal points (the use of the H - E diagrams in the analysis of the existence and stability of solitons is explained in Ref. [24]). It is also obvious from Fig. 2 that the stability interval, in terms of E , shrinks and then disappears with the increase of β (it exists for $\beta = \pm 0.01$, and is absent for $\beta = \pm 0.05$). The latter feature qualitatively resembles that found in numerical simulations of the 2D model with the $\chi^{(2)}$ and self-focusing $\chi^{(3)}$ nonlinearities in Ref. [11], see Fig. 15 in that work.

In Fig. 3 we plot energy E vs wave number k for two representative values of the GVD ratio σ . Note that the soliton solutions bifurcate from unstable 3D NLS solitons of the SH wave V in the cubic medium, which are particular solutions to Eqs. (1) with $U=0$ and $V \neq 0$. The bifurcation points are marked by open circles in Fig. 3. The $k=k(E)$ relation for these unstable solitons $k = -\beta/2 + \text{const} \times \sigma E^{-2}$, with $\text{const} \approx 0.69$ [5], is depicted by blue (light grey) lines in Fig. 3. Full stability of the solitons is determined by eigenvalues λ of small perturbations, that we computed from the equations linearized around the stationary solutions. In Figs. 4(a) and 4(b), we plot the maximum value of the instability gain, $\text{Re}(\lambda)$, as a function of the shifted propagation constant, $k-k_{\text{CO}}$, of the unperturbed STSs, for $\sigma=1$ and three representative values of mismatch β . At $\beta=0$, the stability region, with $\text{Re}(\lambda)=0$, is $0 < k < 0.02$. With $\beta \neq 0$, numerically found stability windows are $0.0064 < k < 0.022$ for $\beta = -0.01$, and $0.0012 < k < 0.017$ for $\beta = 0.01$. The predictions of the linear stability analysis were checked in direct simulations of Eqs. (1), which were run by means

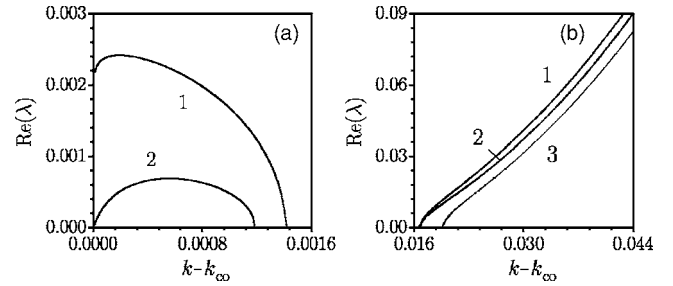


FIG. 4. The largest real part of the perturbation growth rate vs the shifted soliton's wave number $k-k_{\text{CO}}$, in the model with $\sigma=1$. Labels 1, 2, and 3 correspond to $\beta = -0.01$, $\beta = 0.01$, and $\beta = 0$, respectively. Panels (a) and (b) separately display the instability growth rates near the left and right edges of stability windows. There is no curve with label 3 in the left panel, as the stability region for $\beta=0$ starts at $k-k_{\text{CO}}=0$.

of the standard Crank-Nicholson scheme. The initial conditions for perturbed solitons were taken as $u(Z=0) = U(X, Y, T)(1 + \epsilon Q)$, $v(Z=0) = V(X, Y, T)(1 + \epsilon Q)$, where (U, V) is a stationary STS solution constructed as described above, ϵ is a small perturbation amplitude, and Q was either a random variable uniformly distributed in interval $[-0.5, 0.5]$, or simply $Q=1$ (uniform perturbation). This way, we have checked that all STSs that were predicted above to be stable or unstable, as per the eigenvalues of small perturbations, are stable/unstable indeed in direct simulations. In particular, unstable solitons either decay or suffer collapse. The robustness of stable solitons is illustrated by self-trapping of a 3D soliton from an arbitrary spatiotemporal pulse. A typical example of that is shown in Fig. 5 for an *isotropic* Gaussian input, which generates a stable ellipsoidal soliton, adjusted to $\sigma \neq 1$.

In conclusion we have demonstrated that the quadratic ($\chi^{(2)}$) interaction between fundamental-frequency and second-harmonic waves in bulk dispersive media, combined with the self-focusing cubic nonlinearity, give rise to a family of 3D spatiotemporal optical solitons, which may be stable, despite the presence of the supercritical collapse in the model. The stability region of the solitons was, at first,

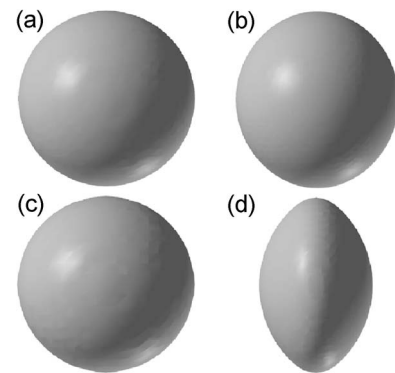


FIG. 5. Self-trapping of the 3D soliton for $\sigma=0.1$ and $\beta=0$. (a) and (c) The Gaussian input in the FF and SH components; (b) and (d) the FF and SH soliton components at $Z=20000$.

predicted on the basis of the Vakhitov-Kolokolov criterion, then confirmed by the computation of the corresponding stability eigenvalues, and finally verified in direct simulations. The physical relevance of the results is emphasized by the fact that optical $\chi^{(2)}$ materials, available to the experiment, always feature the self-focusing Kerr nonlinearity [11].

This work was partially supported by the Government of Spain through Grant No. BFM 2002-2861, by the Ramon-y-Cajal and Juan de la Cierva programmes, by Deutsche Forschungsgemeinschaft (DFG), Bonn, and by the Israel Science Foundation through the Center-of-Excellence Grant No. 8006/03.

-
- [1] Yu. S. Kivshar and G. P. Agrawal, *Optical Solitons: From Fibers to Photonic Crystals* (Academic Press, San Diego, 2003).
- [2] B. A. Malomed, *Soliton Management in Periodic Systems* (Springer, New York, 2006).
- [3] Y. Silberberg, *Opt. Lett.* **15**, 1282 (1990).
- [4] B. A. Malomed *et al.*, *J. Opt. B: Quantum Semiclassical Opt.* **7**, R53 (2005).
- [5] L. Bergé, *Phys. Rep.* **303**, 260 (1998).
- [6] I. Towers and B. A. Malomed, *J. Opt. Soc. Am. B* **19**, 537 (2002).
- [7] M. Matuszewski *et al.*, *Phys. Rev. E* **70**, 016603 (2004).
- [8] N. K. Efremidis *et al.*, *Phys. Rev. E* **66**, 046602 (2002); J. W. Fleischer *et al.*, *Nature* (London) **422**, 147 (2003); B. B. Baizakov *et al.*, *Europhys. Lett.* **63**, 642 (2003); D. Neshev *et al.*, *Phys. Rev. Lett.* **92**, 123903 (2004).
- [9] D. Edmundson and R. H. Enns, *Opt. Lett.* **17**, 586 (1992); N. Akhmediev and J. M. Soto-Crespo, *Phys. Rev. A* **47**, 1358 (1993); R. McLeod *et al.*, *ibid.* **52**, 3254 (1995).
- [10] B. A. Malomed *et al.*, *Phys. Rev. E* **56**, 4725 (1997); D. V. Skryabin and W. J. Firth, *Opt. Commun.* **148**, 79 (1998); D. Mihalache *et al.*, *ibid.* **152**, 365 (1998); D. Mihalache *et al.*, *ibid.* **169**, 341 (1999); D. Mihalache *et al.*, *Phys. Rev. E* **62**, 7340 (2000).
- [11] X. Liu *et al.*, *Phys. Rev. Lett.* **82**, 4631 (1999); *Phys. Rev. E* **62**, 1328 (2000).
- [12] M. L. Quiroga-Teixeiro and H. Michinel, *J. Opt. Soc. Am. B* **14**, 2004 (1997).
- [13] I. Towers *et al.*, *Phys. Lett. A* **288**, 292 (2001); B. A. Malomed *et al.*, *Physica D* **161**, 187 (2002); D. Mihalache *et al.*, *Phys. Rev. Lett.* **88**, 073902 (2002).
- [14] E. V. Kazantseva, A. I. Maimistov, and B. A. Malomed, *Opt. Commun.* **188**, 195 (2001).
- [15] I. Towers *et al.*, *Phys. Rev. E* **63**, 055601(R) (2001); D. Mihalache *et al.*, *ibid.* **66**, 016613 (2002).
- [16] L. Torner and D. V. Petrov, *Electron. Lett.* **33**, 608 (1997); W. J. Firth and D. V. Skryabin, *Phys. Rev. Lett.* **79**, 2450 (1997); D. V. Petrov *et al.*, *Opt. Lett.* **23**, 1444 (1998).
- [17] O. Bang *et al.*, *Opt. Lett.* **22**, 1680 (1997); O. Bang *et al.*, *Phys. Rev. E* **58**, 5057 (1998).
- [18] C. Etrich *et al.*, *Prog. Opt.* **41**, 483 (2000); A. V. Buryak *et al.*, *Phys. Rep.* **370**, 63 (2002).
- [19] L. Khaykovich and B. A. Malomed, *Phys. Rev. A* **74**, 023607 (2006).
- [20] V. E. Zakharov and E. A. Kuznetsov, *Zh. Eksp. Teor. Fiz.* **91**, 1310 (1986); [*Sov. Phys. JETP* **64**, 773 (1986)].
- [21] A. A. Kanashov and A. M. Rubenchik, *Physica D* **4**, 122 (1981).
- [22] L. Torner *et al.*, *Phys. Rev. Lett.* **77**, 2455 (1996); C. Etrich *et al.*, *Phys. Rev. E* **55**, 6155 (1997); D. Mihalache *et al.*, *Opt. Commun.* **137**, 113 (1997); L. Torner *et al.*, *J. Opt. Soc. Am. B* **15**, 1476 (1998); R. H. J. Grimshaw *et al.*, *Physica D* **152**, 325 (2001); D. Mihalache *et al.*, *Opt. Eng. (Bellingham)* **35**, 1616 (1996); C. Etrich *et al.*, *Opt. Quantum Electron.* **30**, 881 (1998).
- [23] M. G. Vakhitov and A. A. Kolokolov, *Radiophys. Quantum Electron.* **16**, 783 (1973).
- [24] F. V. Kusmartsev, *Phys. Rep.* **183**, 1 (1989). A. Ankiewicz and N. Akhmediev, *IEE Proc.: Optoelectron.* **150**, 519 (2003).